

Modeling shotcrete mix design using artificial neural network

Khan Muhammad^{*}, Noor Mohammad^a and Fazal Rehman^b

Department of Mining Engineering, University of Engineering & Technology, Peshawar, KP, Pakistan

(Received October 25, 2012, Revised August 31, 2014, Accepted November 25, 2014)

Abstract. “Mortar or concrete pneumatically projected at high velocity onto a surface” is called Shotcrete. Models that predict shotcrete design parameters (e.g. compressive strength, slump etc) from any mixing proportions of admixtures could save considerable experimentation time consumed during trial and error based procedures. Artificial Neural Network (ANN) has been widely used for similar purposes; however, such models have been rarely applied on shotcrete design. In this study 19 samples of shotcrete test panels with varying quantities of water, steel fibers and silica fume were used to determine their slump, cost and compressive strength at different ages. A number of 3-layer Back propagation Neural Network (BPNN) models of different network architectures were used to train the network using 15 samples, while 4 samples were randomly chosen to validate the model. The predicted compressive strength from linear regression lacked accuracy with R^2 value of 0.36. Whereas, outputs from 3-5-3 ANN architecture gave higher correlations of $R^2 = 0.99, 0.95$ and 0.98 for compressive strength, cost and slump parameters of the training data and corresponding R^2 values of $0.99, 0.99$ and 0.90 for the validation dataset. Sensitivity analysis of output variables using ANN can unfold the nonlinear cause and effect relationship for otherwise obscure ANN model.

Keywords: ANN; shotcrete design; admixtures; sensitivity analysis

1. Introduction

Shotcrete is preferred support for underground and surface mining/civil structures compared to conventional rock bolting and mesh supported systems for its ease in plastering, high productivity, lower underground maintenance requirements, lesser labor requirements, and cost effectiveness (Leung *et al.* 2005, Leung *et al.* 2006, Hoek 2007). Environmental and engineering factors encourage the use of industrial waste or by-products e.g. slag, silica fume, and fibers as admixtures in shotcrete which improve various shotcrete properties. Silica fume increases the density (Rasa *et al.* 2009) adhesion and cohesion properties (Maimberg 1993) of shotcrete which results in lesser rebound during shotcrete layering and greater compressive strength. Addition of steel fibers prevent cracks formation due to different shrinkage rates in a shotcrete layer (Leung *et al.* 2006). It makes shotcrete highly resistant to impact energy released during blasting, seismic activity and similar destabilizing factors in underground environment (Banthia *et al.* 1999). Appropriate

^{*}Corresponding author, Assistant Professor, E-mail: khan.m@uetpeshawar.edu.pk

^aProfessor, Head of Department, Ph.D. E-mail: chair_min@nwfpuet.edu.pk

^bPostgraduate Student, Department of Mining Engineering UET Peshawar

mixing of silica fume and steel fibers in shotcrete is of key significance to improve rebound, compressive and flexural strength (Morgan and Wolsiefer 1991).

However, the selection of appropriate shotcrete mix design is often left to the experience of the shotcreting crew who rely on lengthy and time consuming trial and error procedures (Maimberg 1993). Alternatively, developing prediction models for such processes from experimental data could save extensive time consumed during trial and error based design. For this purpose, highly adaptive models such as Artificial Neural Networks (Sonmez *et al.* 2006) are most suitable that can encompass the nonlinearity between output design parameters and mixing ingredients/admixtures. ANN is preferred for its prediction accuracy compared to other methods such as multivariate linear regression (Atici 2011) or fuzzy logic (Özcan *et al.* 2009). It has been successfully used in engineering applications such as development of neural network based rock mass classification system (Sonmez *et al.* 2006, Yang and Zhang 1998), prediction of vibration for quarry blasting design (Khandelwal and Singh 2009), prediction of aggregate quality (Huang, 1999). Many researchers (Tavakkol *et al.* 2013, Eredm *et al.* 2013, Shah and Ribakov 2011, Yeh 1998, Ni and Wang 2000, Dias and Pooliyadda 2001, Ji *et al.* 2006, Öztaş *et al.* 2006, Altun *et al.* 2008, Rasa *et al.* 2009, Bilgehan and Turgut 2010) have used ANN to predict compressive strength, flexural strength and slump of concrete from different proportions of primary mixing components i.e. water, cement, aggregate sizes and a variety of admixtures such as steel fibers silica fume, fly ash and blast furnace slag. However, characteristics of shotcrete are different from ordinary concrete in many ways: such as the description of coarse aggregate size is smaller in shotcrete than in concrete; temperature and humidity are of less concern during underground applications of shotcrete and early compressive strength is of more importance in shotcrete than in ordinary concrete (Xie *et al.* 2011). Noticeably, shotcrete design problems are of inverse nature (Atici 2011) since we often require to determine mixing proportions of ingredients for already identified design parameters such as compressive strength. Yet, the prediction models still save considerable experimentation time and are therefore popularly in use within the industry. In this paper ANN is used to predict properties of shotcrete i.e. compressive strength, slump and cost as 'output variables' using varying mixing proportions of water content, silica fume and steel fibers, as 'inputs' with fixed quantities of aggregate and cement.

The next three sections present, overview of: multivariate regression, Back Propagation Neural Network (BPNN) model and modeling shotcrete mix design, then the experimental setup section is presented. After application of ANN on the data and sensitivity analysis, the results and discussion section is presented. The paper ends with the conclusion section.

2. Multivariate linear regression

Knowing the “ n ” input variables, any j th output variable in multiple linear regression, is obtained from a linear combination of the input variables and their corresponding coefficients.

$$y_j = c_0 + c_1 X_1 + c_2 X_2 + \dots + c_n X_n$$

where c_0 is the regression constant and c_1, c_2, \dots, c_n are the regression parameters for associated input variables $X_1, X_2, X_3, \dots, X_n$. The coefficients are estimated by minimizing the mean squared error between samples and regression line through well-established statistical least square estimation method. The regression constant and regression parameters are given as:

$$P_j = [X^T X]^{-1} X^T y_j, \text{ where:}$$

$X = (N \times n+1)$ matrix of the n dimensional input variables plus a column of unity

$y_j = (N \times 1)$ output variables vector

N = total number of samples

The regression parameters c_i for any i th input variable and a constant c_0 are given by:

$$c_i = [P_1, P_2, \dots, P_n] \text{ , for } i = 1, 2, \dots, n \text{ and } c_0 = [P_{n+1}]$$

3. Artificial Neural Networks

Artificial Neural Network (ANN) is a layered set of node connections that emulate human nervous system (Hopfield 1988) and learn to adapt itself to the output data by changing the corresponding weights connecting different nodes or neurons in subsequent layers. For a simple 3 layer architecture with input layer $l = 0$, hidden layer $l = 1$ and output layer $l = L=2$ having K^l neurons in l th layer where each neuron a_j^l represents output value of any j th neuron in the l th layer (see Fig. 1). Additionally, every layer except the output layer has a 0th bias neuron whose output a_0^l in any case is equal to unity.

Each neuron j , $\forall j=0,1,2,\dots,K^l$ in layer l , is connected through weights w_{ij}^l to the i th neuron $\forall i=1,2,\dots,K^{l+1}$ in the $(l+1)$ th layer. As input data is fed into the input layer, the K^0 dimensional inputs of any p th sample plus the bias node value of unity are simply passed on to the next layer $l = 1$. The output of the i th neuron in the next layer $l = 1$ is given as: $z_i^{l+1} = z_i^1 = \sum_j^{K^0} a_j^0 w_{ij}^0$ where $j = 0, \dots, K^0$. The final output a_i^{l+1} of the i th neuron in $(l+1)$ th layer is nonlinear activation function (e.g. sigmoid function) of the previously obtained weighted linear combination term z_i^{l+1} i.e. $a_i^{l+1} = a_i^1 = f(z_i^1) = \frac{1}{(1 + e^{-z_i^1})}$ for all $i=1,2,\dots,K^1$. The same procedure is adopted to obtain outputs a_i^2 for all the nodes in the second layer, and onwards, till the outputs for all K^2 neurons in the output layer $L=2$ are achieved; this completes a forward pass.

3.1 Back propagation neural network

Learning takes place by updating the connecting weights after the error term for each output node is determined and redistributed backwards to update the connecting weights. The objective function, i.e. Sum of Squared Error (SSE) = $\sum_p^N \sum_i^{K^2} (y_{pi} - o_{pi})^2$ ought to be minimized such that; ignoring the term p for N samples, k th node output $o_k = a_k^2 = f(a_k^2)$ of the output layer, is closest to the "actual" output y_k . Since the activation function is a function of weighted linear combination of outputs of preceding layers, the connection weights are to be updated in order to minimize the error function SSE. The weights updating term " Δw_{kj}^1 ", connecting j th term of $l=1$ to

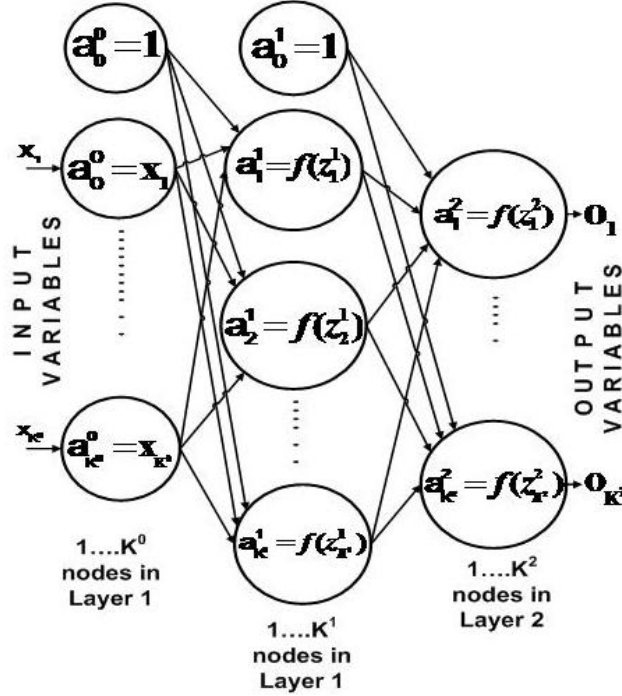


Fig. 1 A general 3 layer ANN design

k th node of output layer $l=2$, is directly proportional to the error term $\delta_k^2 = \frac{\partial E}{\partial w_{kj}^1}$ of k th node in output layer $l=2$. For the sigmoid function, this term can be obtained as (Mehrotra *et al.* 1997):

$$\frac{\partial E}{\partial w_{kj}^1} = -2 \underbrace{(y_k - o_k) o_k (1 - o_k)}_{\delta_k^2} a_j^1$$

The updated weights w^{l*} connecting the hidden layer $l=1$ to the output layer $l=2$ is determined by $w^{l*} = w^l + \alpha \Delta w^l + \eta \delta_k^2 a_j^1$. Where, $\Delta w^l = \eta \delta_k^2 a_j^1$ is the change in weights term, η = learning rate for weights update, Δw^l is the previous weight update term α is the momentum term, with a predefined value chosen within range of 0-1. The term $\alpha \Delta w^l$ smoothen the learning process and increases speed of optimization (Lecun *et al.* 1998). Similarly the term $\frac{\partial E}{\partial w_{ji}^0}$ is

given as: $\Delta w_{ji}^0 = \frac{\partial E}{\partial w_{ji}^0} = -2 \underbrace{\sum_k (y_k - o_k) o_k (1 - o_k) w_{kj}^1}_{\mu_j^1} \times a_i^0$, when using the sigmoid

function. The final equation for updated weights w^{0*} , connecting layer 0 to layer 1, is given as:

$$w^{0*} = w^0 + \alpha \Delta w^0 + \eta \mu_j^1 a_i^0$$

A learning rate is chosen, within a range of 0-1, however, lower value leads to slower

convergence, while too high value makes the learning process jerky, making it difficult to meet the convergence criteria. The variance of fluctuations around a local minimum is directly proportional to the learning rate (Lecun *et al.* 1998). After new weights are determined, the feed forward step is performed again to recalculate the values of output nodes. When this error is less than a predefined threshold value or if a predefined number of epochs is exhausted the final weights are fixed and the network is finally trained; otherwise, the procedure is repeated.

4. Modeling shotcrete mix design

Wet mix shotcreting method is preferred due to its ease in homogenous mixing, less rebound, greater productivity, lower dust and cost compared to dry mix process (Morgan and Wolsiefer 1991, Maimberg 1993, Armelin and Banthia 1998). Aggregate oversize (> 8 mm) is avoided to prevent plugging of the hose or nozzle and high rebound especially in presence of lower water content and airflow (Armelin and Banthia 1998). The use of accelerators for early strength of shotcrete (Prudhicio 1998) may be avoided, since it can affect the quality of shotcrete due to uneven distribution of accelerators, resulting in different settling times of shotcrete layers (Jolin and Beaupré 2003).

Flexural strength, toughness and compressive strength are commonly reported strength parameters during shotcrete design (Chan *et al.* 2002, Leung *et al.* 2005). Compressive strength considers the structural capacity and durability of shotcrete for different applications (Chan *et al.* 2002). Compressive strength of shotcrete and concrete is important parameter for categorizing different shotcretes according to design requirements in different environments (Hakim *et al.* 2011, Alilou and Teshnehlab 2010). Slump is another important parameter that effects pumpability and greater build up thickness during a single shotcrete layering thus increasing productivity (Jolin and Beaupré 2003). However, excessive slump increases rebound causing loss of material and thin layering (Chan *et al.* 2002), however, when slump is too small it may also choke the nozzle (Chan *et al.* 2002). In some cases, e.g. for deep mines when shotcrete is transported through gravity flow in pipes, a surface slump spread of 25-28 inches is allowed (Millete and Lessard 2007). Increase in slump also improves the pumpability of shotcrete; in such cases high initial air content (10-20%) is needed to provide maximum buildup thickness through the “slump killing effect” (Jolin and Beaupré 2003).

4.1 Data collection before modeling

Several design of experiments methods (Wahid and Nadir 2013) are available for carrying out experimental studies to get optimum number of experiments. When the individual affect of factor variables is dominant compared to the interactive affect of factor variables, the simplest one factor at a time based experimental model is preferred (Frey *et al.* 2003), which often leads to smaller number of experiments. Recently, several researchers (Avunduk *et al.* 2014, Baskar *et al.* 2011, Kalyani *et al.* 2008, Ko and Shang 2011, Mohammed and Hamza 2011, Sayadi *et al.* 2013) have successfully applied ANN to develop models using small datasets. However, thoughtful analysis of the results is needed to assess the soundness of the model through suitable quantitative and qualitative measures.

5. Experimental setup

This research work was carried out at the department of Mining Engineering, University of Engineering and Technology Peshawar Pakistan. Water content and two admixtures: silica fume and steel fibers were chosen as input parameters. The specifications of steel fibers used in this study are given in Table 1. All the remaining samples equally contained 500 Kg/m³ of Type I (ASTM C 150) Ordinary Portland cement, 725 Kg/m³ of fine aggregate (0-1 mm) and 595 Kg/m³ of coarse aggregate (4-8 mm). The output design parameters considered were compressive strength, cost and slump of shotcrete.

Basic components of shotcrete; aggregate, water and cement were mixed along with varying quantities of silica fume and steel fibers using Aliva AL385 shotcrete spraying machine, with 50mm nozzle outlet and constant air supply at pressure of 6 bar. Shotcrete design specifications of ACI-506R-90 (1995) were followed during preparation of shotcrete. The fine and course aggregates were collected from Sakhi Sarwar, Dera Ghazi Khan District of Punjab in Pakistan. Shotcrete sample mixtures were prepared in 19 vertically placed separate wooden panels (24in width, 24 in. length and depth of 9 in.) that were sprayed with shotcrete keeping the nozzle position horizontal at a distance of 1m from the panel as per ASTM C 1140-03a. The chemical composition of water used is shown in Table 2. The quantity of steel fibres and silica fume were changed as percentage of cement used in mix design.

The cost of the admixtures together with aggregate, cement and water was calculated. Slump of the shotcrete mix was determined as per ASTM C143M using a 30cm long standard slump cone with 20cm bottom diameter and 10cm top diameter. Shotcrete was sprayed from the top in three intervals, each of 10cm height. Each layer of shotcrete was stirred using a tamping rod before adding the next layer, a final layer filled the cone to the top where it was leveled with upper end of cone by drawing off the extra shotcrete. After cleaning the surroundings, the cone was lifted smoothly by applying even pressure at both ends and the slump in shotcrete was measured.

Before measuring the compressive strength, the panels were kept in underground conditions for 28 days at a temperature of 20-25° C and 65-70 % humidity. Three cores were taken from each panel after 7, 14 and 28 days. The core was prepared to have Length to Dia ratio equivalent to 2 as per ASTM C 42/C 42M-03. The length of 3.5 inches diameter core was reduced from 9 inches (panel depth) to 7 inches after sawing the extra part using concrete cutter. Compressive strength tests were conducted at the rock mechanics laboratory Department of Mining Engineering University of Engineering and Technology Peshawar, Pakistan. The average compressive strength of these 3 cores of specific ages from each panel was reported as the compressive strength of particular shotcrete mix at that age. 19 shotcrete mixtures are obtained by varying one factor at a time from water, silica fume and steel fibers that are shown in Table 3 along with their corresponding output parameter values.

Table 1 Specifications of steel fibers used in this study

| | |
|------------------|-----------------|
| ASTM A820 | Type I |
| Material | Cold drawn wire |
| Tensile strength | Over 1,000 MPa |
| Aspect ratio | 45 ~ 75 |
| Length | 30 - 35mm |

Table 2 Analysis of water sample

| | |
|--|-----|
| pH | 7.1 |
| Total Hardness (ppm as CaCO ₃) | 257 |
| Calcium (ppm) | 20 |
| Magnesium (ppm) | 17 |
| Total Dissolved Salts (ppm) | 502 |
| Chlorides (ppm) | 23 |
| Sulphates (ppm) | 70 |

Table 3 Data collected from experimentation design

| Water (Kg/m ³) | Steel Fibres (Kg/m ³) | Quantity of Silica Fume (Kg/m ³) | Slump (cm) | 7th Day Compressive Strength (Psi) | 14th Day Compressive Strength (Psi) | 28th Day Compressive Strength (Psi) | Cost /m ³ (Pak Rs) |
|----------------------------|-----------------------------------|--|------------|------------------------------------|-------------------------------------|-------------------------------------|-------------------------------|
| 280 | 0 | 0 | 12 | 1620 | 1701 | 1750 | 2769 |
| 290 | 0 | 0 | 13 | 2003 | 2103 | 2174 | 2769 |
| 300 | 0 | 0 | 17 | 2053 | 2197 | 2245 | 2769 |
| 310 | 0 | 0 | 20 | 1607 | 1703 | 1811 | 2769 |
| 320 | 0 | 0 | 22 | 1519 | 1625 | 1702 | 2769 |
| 300 | 13 | 0 | 17 | 3249 | 3574 | 3640 | 3679 |
| 300 | 20 | 0 | 15 | 3464 | 3671 | 3701 | 4169 |
| 300 | 27 | 0 | 14 | 3015 | 3656 | 3845 | 4659 |
| 300 | 34 | 0 | 14 | 2641 | 2852 | 3040 | 4948 |
| 300 | 40 | 0 | 13 | 2194 | 2325 | 2647 | 5569 |
| 300 | 0 | 20 | 16 | 2594 | 2801 | 2950 | 3169 |
| 300 | 0 | 30 | 16 | 2711 | 2982 | 3154 | 3369 |
| 300 | 0 | 40 | 15 | 2945 | 3122 | 3462 | 3569 |
| 300 | 0 | 50 | 14 | 2992 | 3201 | 3397 | 3769 |
| 300 | 0 | 60 | 10 | 1590 | 1733 | 1971 | 3969 |
| 300 | 13 | 10 | 17 | 3049 | 3314 | 3510 | 3879 |
| 300 | 13 | 20 | 16 | 3357 | 3572 | 3780 | 4079 |
| 300 | 13 | 30 | 13 | 3156 | 3431 | 3660 | 4279 |
| 300 | 13 | 40 | 11 | 3052 | 3354 | 3442 | 4479 |

6. Prediction models using multivariate linear regression

Multivariate regression parameters, associated with input variables: water content (WC), steel fibres (St) and silica fume (SF); were derived using least square estimation. The equations for compressive strength (C. Strength), cost and slump are derived as:

$$\text{C. Strength} = 0.34 - 0.09 \times \text{WC} + 0.68 \times \text{St} + 0.44 \times \text{SF}$$

$$\text{Cost} = 0.009 + 0 \times \text{WC} + 0.958 \times \text{St} + 0.425 \times \text{SF}$$

$$\text{Slump} = 0.17 + 0.9 \times \text{WC} - 0.344 \times \text{St} - 0.45 \times \text{SF}$$

Results indicated prediction of compressive strength was poor with R^2 value of 0.36 while that of slump and cost was relatively high at 0.85 and 0.89. The lower correlation was due to the presence of nonlinear relationship between compressive strength and input parameters; therefore, to achieve a better fit, application of ANN was essential.

7. Application of ANN model for predicting compressive strength, cost and slump references

First, the complete dataset "X", including all the input and output variables were range transformed i.e. $(X - X_{\min}) / (X_{\max} - X_{\min})$. The samples were separated into two sets, 15 samples were used to train the ANN network model, while 4 were randomly chosen to validate the network. The ANN code was coded in MATLAB after detailed explanation by various authors (Fausett 1993, Mehrotra *et al.* 1997). A number of nodes in the hidden layer were tried to obtain various 3-layered architectures (3-2-3, 3-3-3.....) that were first trained using batch mode and then using online mode. The learning rate and momentum for online training were set to 0.2 and 0.5, while these values were fixed to 0.3 and 0.5 correspondingly during batch mode training. The activation function in all cases was sigmoid function and objective function was Sum of Squared Error (SSE). In each case, the training was set to terminate at 30,000 iterations or if the SSE was less than or equal to 0.0001.

Table 4 The sum of square errors for training (SSE), and validation data (SSE-V) along with corresponding correlation coefficients for different network architectures trained in batch mode

| Network Architectures | SSE | SSE-V | Training R square | | | Validation R square | | |
|-----------------------|------|-------|-------------------|------|-------|---------------------|------|-------|
| | | | C Strength | Cost | Slump | C Strength | Cost | Slump |
| 363 | 0.12 | 0.07 | 0.99 | 0.99 | 0.97 | 0.99 | 0.99 | 0.90 |
| 353 | 0.13 | 0.05 | 0.98 | 0.99 | 0.98 | 0.99 | 0.99 | 0.93 |
| 343 | 0.21 | 0.05 | 0.97 | 0.99 | 0.95 | 0.99 | 0.99 | 0.93 |
| 333 | 0.36 | 0.06 | 0.95 | 0.99 | 0.90 | 1.00 | 1.00 | 0.79 |
| 323 | 0.77 | 0.05 | 0.85 | 0.97 | 0.89 | 1.00 | 1.00 | 0.93 |

Table 5 The sum of square errors of training (SSE), and validation data (SSE-V) with corresponding correlation coefficients of output variables for different network architectures trained in online mode

| Network Architectures | SSE | SSE-V | Training R square | | | Validation R square | | |
|-----------------------|------|-------|-------------------|------|-------|---------------------|------|-------|
| | | | C Strength | Cost | Slump | C Strength | Cost | Slump |
| 373 | 0.06 | 0.09 | 1.00 | 0.99 | 0.98 | 0.99 | 0.99 | 0.90 |
| 363 | 0.05 | 0.06 | 1.00 | 0.99 | 0.99 | 1.00 | 0.99 | 0.92 |
| 353 | 0.07 | 0.06 | 0.99 | 0.99 | 0.99 | 0.99 | 1.00 | 0.94 |
| 343 | 0.10 | 0.09 | 0.99 | 0.99 | 0.98 | 0.99 | 0.98 | 0.89 |
| 333 | 0.25 | 0.07 | 0.99 | 0.96 | 0.94 | 0.99 | 0.99 | 0.91 |
| 323 | 0.52 | 0.09 | 0.92 | 0.96 | 0.91 | 1.00 | 0.97 | 0.92 |

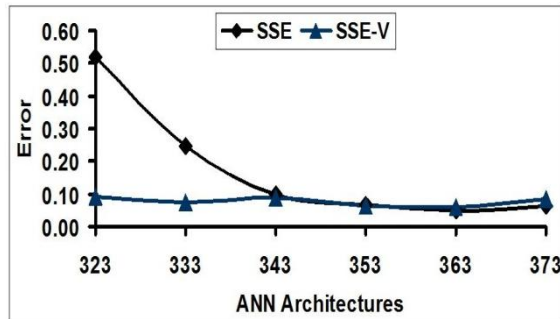


Fig. 2 Comparison of SSE and SSE-V for different network architectures trained in online mode.

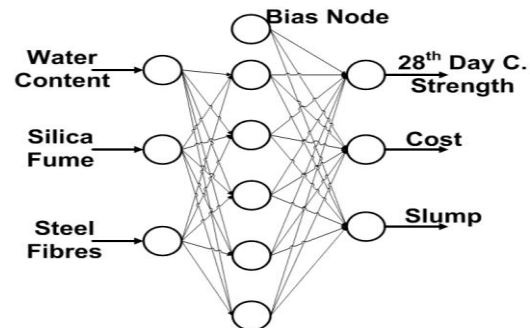


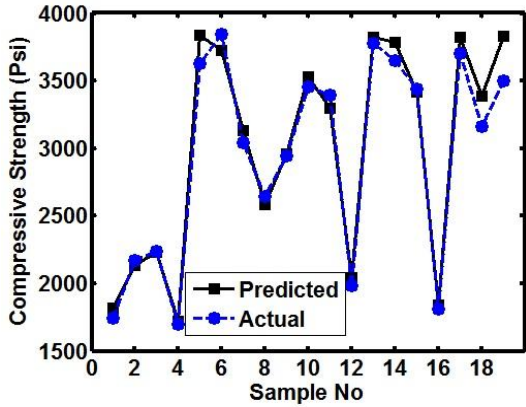
Fig. 3 Final model architecture.

After completion of the training phase, the input parameters of the validation data were fed to all the trained network architectures. The best model architecture was selected by analyzing R^2 values and SSE between predicted and actual outputs of training and validation datasets. Training in batch mode was faster having average training time of 10 sec compared to online training with an average training time of 350 seconds. The sum of square error for validation data 'SSE-V' was lowest i.e. 0.05 for 3-2-3, 3-4-3 and 3-5-3 architecture in batch mode, as seen in Table 4. However, the corresponding SSE were quite high in case of batch mode training compared to the online learning mode as shown in Tables 4-5. In batch learning mode the sum of squared error for training data increased with increase in number of nodes in the hidden layer. However, for validation data, correlation coefficient for slump decreases slightly when number of nodes in hidden layer exceeded beyond 5.

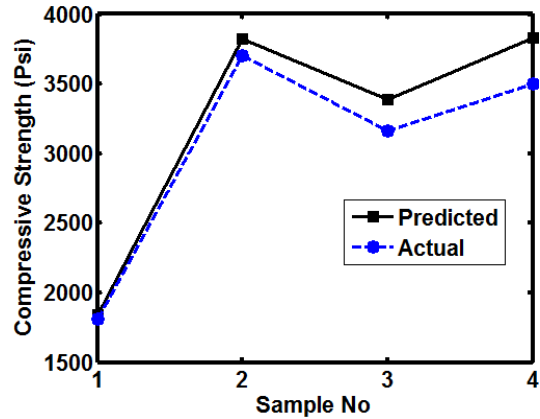
8. Results and discussion

As shown in Fig. 2 the 3-5-3 architecture, trained in online mode, was selected as the best model since it had the lowest training and validation errors i.e. SSE (0.07) and SSE-V (0.06). The results from 3-5-3 architecture (Fig. 3) trained in online learning are shown collectively in Fig. 4. Online learning mode, took longer to train, however, the training SSE was lower than models trained in batch mode. The validation SSE-V increased as the number of nodes in hidden layer exceeded beyond 6 nodes. Further increase in hidden nodes carried no significant improvement in SSE-V and model was prone to over fitting, since SSE-V increased to 0.09 for 3-7-3 architecture (see Table 5). Validation samples 16-19 shown in Figs. 4(a)-(c) show that sufficient variation is present in these samples. Predicted and actual values of the validation samples for the output variables are also shown separately (Figs. 4(d)-(f)) for a closer look of at the prediction accuracy.

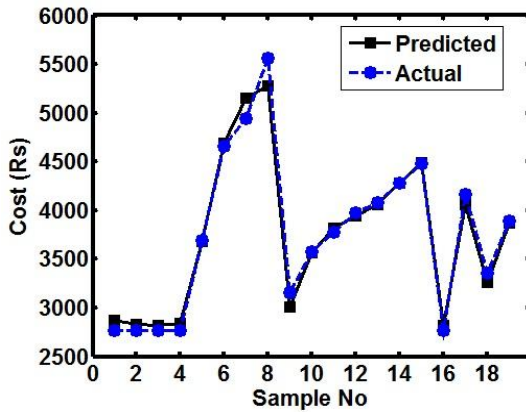
To analyze the effect of mixing components of shotcrete on the output design parameters, Global Relative Strength Effect (GRSE) (Yang and Zhang 1998) was determined that are shown in Table 6. Positive GRSE values indicates the corresponding output variable would increase with the increase in that input variable, whereas negative GRSE values represented inverse relationship between the input and output.



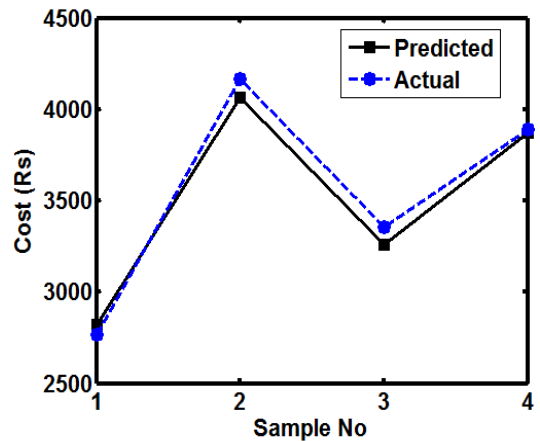
(a) Training and validation of comp. strength



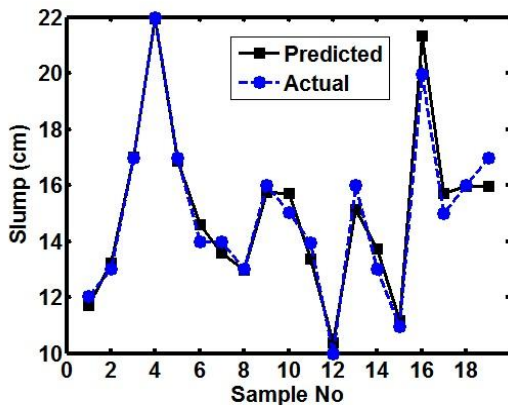
(d) Validation results for comp. strength



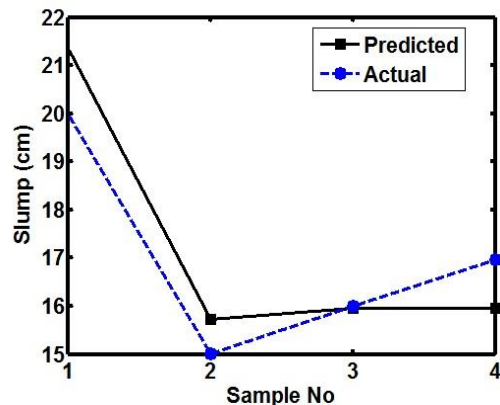
(b) Training and validation of cost



(e) Validation results for cost



(c) Training and validation of slump

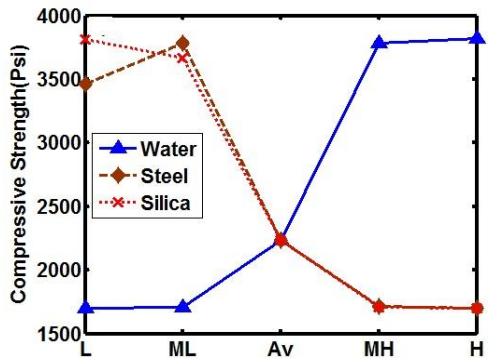


(f) Validation results for slump

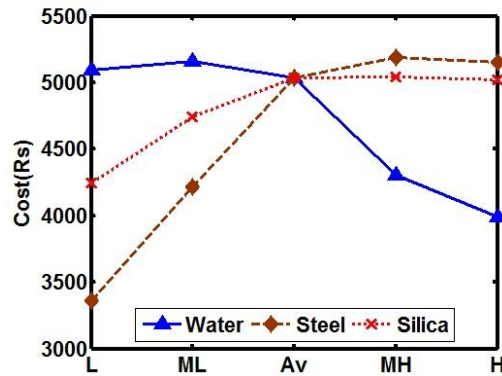
Fig. 4 Comparison of actual and predicted values of 4(a) Compressive Strength, 4(b) Cost and 4(c) Slump using 3-5-3 ANN model, for both training samples (1-15) and validation samples (16-19). A closer look at predicted and actual 4(d) compressive strength, 4(e) cost and 4(f) slump values for validation data is also shown separately

Table 6 GRSE values for 3-5-3 ANN prediction model

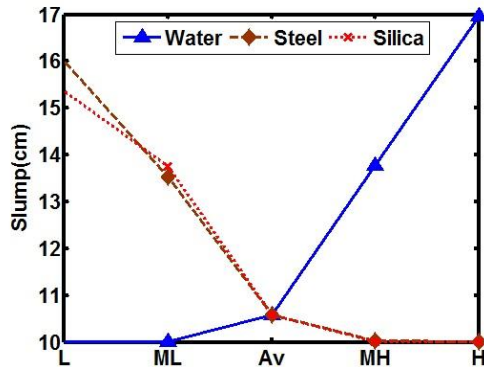
| | C Strength | Cost | Slump |
|---------------|------------|-------|-------|
| Water Content | 1.00 | -0.88 | 1.00 |
| Steel Fibres | -0.72 | 1.00 | -0.61 |
| Silica Fume | -0.74 | 0.49 | -0.77 |



(a) Sensitivity analysis of comp. strength



(b) Sensitivity analysis of cost



(c) Sensitivity analysis of slump

| | Water Kg/m ³ | Steel Kg/m ³ | Silica Kg/m ³ |
|------|----------------------------|----------------------------|-----------------------------|
| L | 280 | 0 | 0 |
| ML | 290 | 11 | 17 |
| Avge | 300 | 22 | 33 |
| MH | 310 | 31 | 47 |
| H | 320 | 40 | 60 |

(d) Respective values of variables used during sensitivity analysis

Fig. 5 Sensitivity analysis results of 3-5-3 ANN model for 5(a) compressive strength, 5(b) cost and 5(c) slump variables through systematic variation of quantities of water (Kg/m³), steel fibres (Kg/m³) and silica fume (Kg/m³) shown in 5(d)

Water content have smaller negative GRSE value for cost and higher positive value for slump indicating as the amount of water is increased, it has decreasing effect on cost and increasing effect on slump. Steel and silica fume with higher positive GRSE values for cost and negative values for slump show their increase will have direct positive effect on cost and reduce slump. However, positive GRSE values of water content and negative value of silica fume and steel fibres indicated compressive strength increased with increase in water and decreased with addition of silica fume and/or steel fibres. This needed further investigation; at best through sensitivity analysis using the ANN model, i.e. changing one input variable systematically for a range of values, keeping other

input variables constant at some acceptable mid-range value.

Five different values for each input variable i.e. Lowest (L); Mid-point between Avg value and Lowest value (ML); Avg value (Av); Mid-Point between Avg value and Highest value (MH) and finally the Highest value (H) were calculated. These values, as shown in Fig. 5(d) were fed into the neural network model for one input variable at a time, systematically; from lowest to highest value while keeping all the other input variables constant at their respective Avg values. The results indicated that variation in inputs for cost and slump complied with GRSE values presented earlier, since the trend was somewhat linear as shown in Figs. 5(b)-(c). However, sensitivity analysis for compressive strength elaborated nonlinearity within the system (see Fig. 5(a)) that was not explained by GRSE analysis.

Sensitivity analysis revealed that silica fume and steel fibres are the major factors responsible for increase in compressive strength; this fact is well established from the literature. Compressive strength sensitivity (Fig. 5(a)) to shotcrete mixtures having L, i.e. 0 Kg/m³ steel fibres indicated that higher compressive strength (3450 Psi) was due to the presence of Avg quantities of Silica fume i.e. 33 Kg/m³ and Water content i.e., 300 Kg/m³.

Sensitivity analysis further suggested that keeping these values constant, a little increase in quantity of steel fibres to ML i.e. 11 Kg/m³, caused increase in 28th day compressive strength value to 3780 Psi which decreased rapidly when steel fibres exceeded from 11 Kg/m³ in the mixture. Silica fume sensitivity line at point L (with no silica fume) showed maximum value for compressive strength i.e. 3815 Psi due to the presence of average quantity of steel fibers i.e. 33 kg/m³. Compressive strength further decreased to 3670 Psi as silica fume value exceeded to ML i.e. 17 Kg/m³. This decreasing trend with addition of more water could be due to unbalance in water to binder ratio, since water quantity was constant at 300 Kg/m³. Similar behavior was indicated by the water sensitivity line, which showed that compressive strength increased with water, that could be due to presence of higher quantity of silica fume at Avg value i.e. 33 Kg/m³ that acts as binding agent (Siddique and Khan 2011), more water was required to achieve the appropriate water to binder ratio for higher compressive strength (Katkhuda *et al.* 2009, Rao 2001). This is further revealed by lower compressive strength of shotcrete i.e. 2230 Psi when all the inputs have average quantities within the shotcrete mixture i.e. 300 Kg/m³ water, 22 Kg/m³ steel fibres and 33 Kg/m³ silica fume. Hence, sensitivity analysis suggested that higher quantity of water 310-320 Kg/m³ would be needed to balance the increase in volume of silica fume + steel fibers content. However, this increase in water also results in higher slump which requires further study, since lower air pressure/content may also be responsible for higher slump due to the absence of the "slump killing effect" (Jolin and Beaupré 2003). The sensitivity analysis using the ANN model showed the cause and effect relationship for the given range of input and output variables. It further suggests investigating ANN models that can incorporate the effect of air content on the output variables and also take into account other important output parameters such as rebound in shotcrete mix design.

9. Conclusions

The results show ANN models perform better than linear regression while predicting shotcrete mix design. The online mode training gave better training results, however, taking longer training time compared to batch mode learning. The 3-5-3 architecture ANN model trained in online mode was retained as best model giving a sum of squared error of 0.07 and 0.06 for training and

validation datasets respectively. The sensitivity analysis by varying one variable at a time is beneficial to extract nonlinear relationship for ANN model, since the Global Relative Strength Effect cannot depict the nonlinearity within the input and output variables. Sensitivity analysis revealed compressive strength improved with addition of silica fume and steel fibres; however, most significant parameter for increase in compressive strength was steel fibres. Sensitivity analysis further suggests that higher quantity of silica fume require higher quantity of water to achieve optimum water to binder ratio. A number of new mix design combinations emerged from sensitivity analysis on ANN model; a suitable mix design can be chosen from these options in accordance with specific design needs.

References

- Akgun, D., Demir, C. and Ilki, A. (2010), "Axial behavior of FRP jacketed extended rectangular members constructed with low strength concrete", *The 5th International Conference on FRP Composites in Civil Engineering*, Beijing, China, September.
- Bailey, C. and Yaqub, M. (2012), "Seismic strengthening of shear critical post-heated circular concrete columns wrapped with FRP composite jackets", *Compos. Struct.*, **94**(3), 851-864.
- Bao, X. and Li, B. (2010), "Residual strength of blast damaged reinforced concrete columns", *Int. J. Impact Eng.*, **37**(3), 295-308.
- Belarbi, A. and Bae, S. (2007), "An experimental study on the effect of environmental exposures and corrosion on RC columns with FRP composite jackets", *Compos. Part B-Eng.*, **38B**(5-6), 674-684.
- CEB-FIP (2010), *CEB-FIP*, CEB-FIP Model Code, Lausanne.
- EIGawady, M., Endeshaw, M., McLean, D. and Sack, R. (2010), "Retrofitting of rectangular columns with deficient lap splices", *J. Compos. Constr.*, **14**(1), 22-35.
- Emmanuel, A. and Oladipo, F. (2012), "Investigation of salinity effect on compressive strength of reinforced concrete", *J. Sustain. Dev.*, **5**(6), 74-82.
- Frangou, M., Pilakoutas, K. and Dritsos, S. (1995), "Structural repair/strengthening of RC columns", *Constr. Build. Mater.*, **9**(5), 259-266.
- Fukuyama, K., Higashibata, Y. and Miyauchi, Y. (2000), "Studies on repair and strengthening methods of damaged reinforced concrete columns", *Cement. Concrete. Compos.*, **22**(1), 81-88.
- GB50010-2010 (2010), *GB50010-2010*, Code for design of concrete structures, Beijing.
- Goksu, C., Polat, A. and Ilki, A. (2012), "Attempt for seismic retrofit of existing substandard RC members under reversed cyclic flexural effects", *J. Compos. Constr.*, **16**(3), 286-299.
- Hanjari, K. (2010), "Structural behaviour of deteriorated concrete structures", Ph.D. Dissertation, Chalmers University of Technology, Göteborgs.
- Harajli, M. (2008), "Seismic behavior of RC columns with bond-critical regions: criteria for bond strengthening using external FRP jackets", *J. Compos. Constr.*, **12**(1), 69-79.
- Haroun, M. and Elsanadedy, H. (2005), "Fiber-reinforced plastic jackets for ductility enhancement of reinforced concrete bridge columns with poor lap-splice detailing", *J. Bridge. Eng.*, **10**(6), 749-757.
- Iacobucci, R., Sheikh, S. and Bayrak, O. (2003), "Retrofit of square concrete columns with carbon fiber-reinforced polymer for seismic resistance", *ACI Struct. J.*, **100**(6), 785-794.
- Kalyoncuoglu, A., Ghaffari, P., Goksu, C. and Ilki, A. (2013), "Rehabilitation of corrosion-damaged substandard RC columns using FRP sheets", *Adv. Mat. Res.*, **639-640**, 1096-1103.
- Kent, D. and Park, R. (1971), "Flexural members with confined concrete", *J. Struct. Div.*, **97**(7), 1969-1990.
- Lam, L. and Teng, J. (2003), "Design-oriented stress-strain model for FRP-confined concrete", *Constr. Build. Mater.*, **17**(6), 471-489.
- Li, B. and Lim, C. (2010), "Tests on seismically damaged reinforced concrete structural walls repaired using

- fiber-reinforced polymers”, *J. Compos. Constr.*, **14**(5), 597-608.
- Li, G., Hedlund, S., Pang, S., Alaywan, W., Eggers, J. and Abadie, C. (2003), “Repair of damaged RC columns using fast curing FRP composites”, *Compos. Part B-Eng.*, **34B**(3), 261-271.
- Li, J., Gong, J. and Wang, L. (2009), “Seismic behavior of corrosion-damaged reinforced concrete columns strengthened using combined carbon fiber-reinforced polymer and steel jacket”, *Constr. Build. Mater.*, **23**(7), 2653-2663.
- Manuel, A. and Silva (2011), “Behavior of square and circular columns strengthened with aramidic or carbon fibers”, *Constr. Build. Mater.*, **25**(8), 3222-3228.
- Mazzoni, S., McKenna, F. and Scott, H. (2009), *Open System for Earthquake Engineering Simulation User Command-language Manual*, Pacific earthquake engineering research center, Berkeley, California, USA.
- Ozcan, O., Binici, B. and Ozcebe, G. (2008), “Improving seismic performance of deficient reinforced concrete columns using carbon fiber-reinforced polymers”, *Eng. Struct.*, **30**(6), 1632-1646.
- Ozcan, O., Binici, B. and Ozcebe, G. (2010), “Seismic strengthening of rectangular reinforced concrete columns using fiber reinforced polymers”, *Eng. Struct.*, **32**(4), 964-973.
- Pantazopoulou, S. J., Bonacci, J., Sheikh, S., Thomas, M. and Hearn, N. (2001), “Repair of corrosion-damaged columns with FRP wraps”, *J. Compos. Constr.*, **5**(1), 3-11.
- Pantelides, C., Gergely, J., Reaveley, L. and Volnyy, V. (1999), “Retrofit of RC bridge pier with CFRP Advanced Composites”, *J. Struct. Eng.*, **125**(10), 1094-1099.
- Rousakis, T. and Karabinis, A. (2008), “Substandard reinforced concrete members subjected to compression: FRP confining effects”, *Mater. Struct.*, **41**(9), 1595-1611.
- Saadatmanesh, H., Ehsani, M.R. and Jin, L. (1997a), “Repair of earthquake-damaged RC columns with FRP wraps”, *ACI Struct. J.*, **94**(2), 206-215.
- Saadatmanesh, H., Ehsani, M.R. and Jin, L. (1997b), “Seismic retrofitting of rectangular bridge columns with composite straps”, *Earthq. Spectra.*, **13**(2), 281-304.
- Saadatmanesh, H., Ehsani, M.R. and Li, M.W. (1994), “Strength and Ductility of concrete columns Externally Reinforced with Fiber Composite Strapes”, *ACI Struct. J.*, **91**(4), 434-447.
- Saadatmanesh, H., Ehsani, M.R. and Jin, L. (1996), “Seismic strengthening of circular bridge pier model with fiber composites”, *ACI Struct. J.*, **93**(6), 639-647.
- Seible, F., Priestley, M.J.N., Hegemier, G.A. and Innamorato, D. (1997), “Seismic retrofit of RC columns with continuous carbon fiber jackets”, *J. Compos. Constr.*, **1**(2), 52-62.
- Sheikh, S.A. and Bayrak, O. (2001), “Seismic behaviour of FRP-Retrofitted concrete columns”, *Proceedings of Structures Congress 2001*, Washington D.C., USA, May.
- Sheikh, S.A. and Yau, G. (2002), “Seismic behavior of concrete columns confined with steel and fiber-reinforced polymers”, *ACI Struct. J.*, **99**(1), 72-80.
- Scott, B.D, Park, R. and Priestley, M.J.N (1982), “Stress-strain behavior of concrete confined by overlapping hoops at low and high strain rates”, *ACI Mater. J.*, **79** (1), 13-27.
- Teng, J., Jiang, T., Lam, L. and Luo, Y. (2009), “Refinement of a design-oriented stress--strain model for FRP-confined concrete”, *J. Compos. Constr.*, **13**(4), 269-278.
- Thermou, G.E. and Pantazopoulou, S.J. (2009), “Fiber-reinforced polymer retrofitting of predamaged substandard RC prismatic members”, *J. Compos. Constr.*, **13**(6), 535-546.
- Wei, H., Wu, Z. and Zhang, P. (2010), “Axial experiment on CFRP confined steel reinforced concrete columns with partial deteriorated strength”, *J. Reinf. Plast. Comp.*, **29**(6), 874-882.
- Wei, H., Wu, Z., Guo, X. and Yi, F. (2009), “Experimental study on partial deteriorated strength concrete columns confined with CFRP”, *Eng. Struct.*, **31**(10), 2495-2505.
- Wei, H. (2009), “Compressive performance study on CFRP wrapped concrete columns with partial deteriorated strength”, Ph.D. Dissertation, Dalian University of technology, Dalian.
- Xiao, Y., Wu, H. and Martin, G.R. (1999), “Prefabricated composite jacketing of RC columns for enhanced shear strength”, *J. Struct. Eng.*, **125**(3), 255-264.
- Yalcin, C. and Kaya, O. (2004), “An experimental study on the behavior of reinforced concrete columns using FRP material”, *13th World Conference on Earthquake Engineering*, Vancouver B.C., Canada, August.

- Yalcin, C., Kaya, O. and Sinangil, M. (2008), "Seismic retrofitting of R/C columns having plain rebars using CFRP sheets for improved strength and ductility", *Constr. Build. Mater.*, **22**(3), 295-307.
- Yu, J., Zhang, Y. and Lu, Z. (2014), "Seismic rehabilitation of RC frame using epoxy injection technique tested on shaking table", *Struct. Eng. Mech.* **52**(3), 541-558.
- Yuan, X., Xia, S., Lam, L. and Smith, S.T. (2008), "Analysis and behaviour of FRP-confined short concrete columns subjected to eccentric loading", *J. Zhejiang. Univ- Sc A.*, **1**(9), 38-49.
- Zhu, Z., Ahmad, I. and Mirmiran, A. (2006), "Fiber element modeling for seismic performance of bridge columns made of concrete-filled FRP tubes", *Eng. Struct.*, **28**(14), 2023-2035.

CC